ACS APPLIED MATERIALS & INTERFACES

FORUM ARTICLE

www.acsami.org

Carbon Fiber-Reinforced Cyanate Ester/Nano-ZrW_2O_8 Composites with Tailored Thermal Expansion

Prashanth Badrinarayanan, Mark K. Rogalski, and Michael R. Kessler*

Department of Materials Science and Engineering, Iowa State University, Ames, Iowa 50014, United States

ABSTRACT:

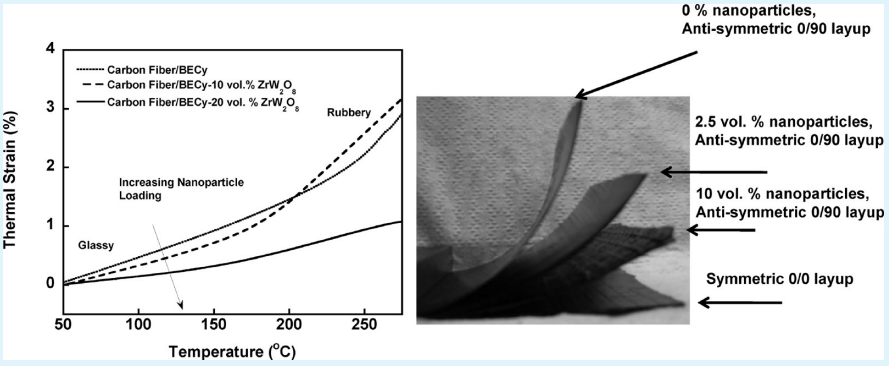

Fiber-reinforced composites are widely used in the design and fabrication of a variety of high performance aerospace components. The mismatch in coefficient of thermal expansion (CTE) between the high CTE polymer matrix and low CTE fiber reinforcements in such composite systems can lead to dimensional instability and deterioration of material lifetimes due to development of residual thermal stresses. The magnitude of thermally induced residual stresses in fiber-reinforced composite systems can be minimized by replacement of conventional polymer matrices with a low CTE, polymer nanocomposite matrix. Zirconium tungstate (ZrW_2O_8) is a unique ceramic material that exhibits isotropic negative thermal expansion and has excellent potential as a filler for development of low CTE polymer nanocomposites. In this paper, we report the fabrication and thermal characterization of novel, multiscale, macro-nano hybrid composite laminates comprising bisphenol E cyanate ester (BECy)/ZrW_2O_8 nanocomposite matrices reinforced with unidirectional carbon fibers. The results reveal that incorporation of nanoparticles facilitates a reduction in CTE of the composite systems, which in turn results in a reduction in panel warpage and curvature after the cure because of mitigation of thermally induced residual stresses.

KEYWORDS: multiscale composites, thermal expansion, zirconium tungstate, residual stress

1. INTRODUCTION

Fiber-reinforced polymer composites are enabling technologies in a wide range of applications from aerospace to microelectronics. Carbon fibers are an excellent choice as fiber reinforcements for high-performance polymer matrix composites (PMCs) because of their low density, high strength, and stiffness. PMCs are often fabricated by impregnating carbon fiber reinforcements with thermosetting polymer resins capable of withstanding elevated service temperatures. The composites are prepared by an elevated temperature curing process, which transforms the thermosetting resin into a rigid, highly cross-linked polymer. When the composite is cooled following the cure, the cured polymer matrix contracts significantly because of the typically high coefficient of thermal expansion (CTE) of polymeric materials. On the other hand, carbon fiber reinforcements exhibit very low or negligible shrinkage due to their comparatively low CTE values. This mismatch in thermal expansivity between the polymer matrix and the carbon fiber reinforcements results in residual stresses in the composite leading to loss of dimensional stability, which can hinder fabrication of parts with precise dimensions. Furthermore, under repeated thermal cycling, the CTE mismatch between the matrix and the fiber reinforcements can lead to thermal fatigue and matrix microcracking causing material failure.[1,2]

A potential strategy to improve the performance and properties of fiber reinforced PMCs involves incorporation of nanoscale filler materials, which can facilitate the desired property enhancements. The use of nanoscale materials to tailor the properties of the fiber reinforced PMCs has led to the development of multiscale, macro-nano hybrid composites, with enhanced thermal, mechanical and electrical properties for multifunctional applications. The two common methods for fabrication of multiscale hybrid composites have involved the use of nanoscale materials to either modify the fibers or the matrix phase. In early work, Thostensen and co-workers[3] reported a 15% improvement in the interfacial shear strength of single fiber epoxy composites upon

Received: August 29, 2011
Accepted: November 1, 2011
Published: November 18, 2011

growth of carbon nanotubes (CNTs) on the carbon fiber surface. Hybrid PMCs prepared through attachment of carbon nanotubes on SiC fiber mats exhibited dramatic enhancements in mechanical and thermal properties.[4] In more recent work, Lin and co-workers[5] developed multifunctional epoxy/carbon fiber composites with improved mechanical properties by growing ZnO nanowires on the surface of carbon fibers. Several researchers have also developed hybrid multiscale composites through inclusion of nanoparticles in the polymer matrix phase, with the vast majority of the efforts being focused on incorporation of nanoscale fillers such as carbon nanotubes,[6−10] carbon nanofibers,[11−13] or silicates[14−16] in epoxy matrices. Furthermore, most previous studies in the literature have focused on improving the mechanical or electrical properties of carbon or glass fiber-reinforced PMCs, whereas the development of multiscale fiber-reinforced PMCs with tailored thermal expansion has not received extensive attention. When PMCs are used in applications such as dimensionally stable mirrors, apertures, telescope components, or microelectronics, residual stresses may also be induced because of their contact with substrates or surfaces with lower values of CTE (e.g., silicon, alumina, glass). The ability to both tailor the overall CTE of the composites and to reduce the mismatch in CTE between the carbon fibers and the polymer matrix would enable mitigation of thermal stresses and also enhance the versatility and service lifetimes of the fiber reinforced composite systems.

Development of hybrid composites through incorporation of negative CTE nanofillers in the polymer phase can reduce the mismatch in CTE between the polymer and fiber phases, while also facilitating an overall low CTE for the composite system. Zirconium tungstate (ZrW_2O_8) is a unique ceramic oxide that exhibits the largest reported isotropic negative thermal expansion (-9×10^{-6} ppm/°C).[17−19] Several researchers have reported substantial reductions in the CTE of polymer resins such as epoxies,[20,21] phenolics,[22] and cyanate esters[23−25] upon incorporation of micrometer size ZrW_2O_8 particles. However, only a few studies[26−28] have examined the potential for development of polymer nanocomposites with negative CTE ZrW_2O_8 particles. Sullivan and co-workers[26] developed polyimide thin films with low CTE values upon incorporation of ZrW_2O_8 nanoparticles synthesized by sol−gel methods. In recent work,[28] we reported the development of bulk polymer nanocomposites containing up to 10 vol. % ZrW_2O_8 nanoparticles dispersed in a low viscosity bisphenol E cyanate ester (BECy) resin. Following full cure, the low viscosity BECy resin is characterized by excellent mechanical properties and high value of glass transition temperature (T_g), which makes it an excellent candidate resin for structural composite applications.[29,30]

This paper describes the fabrication and characterization of novel carbon fiber reinforced BECy/nano-ZrW_2O_8 composite laminates. The objectives of this work are to examine the effect of nanoparticle loading on both the thermal expansion of the symmetric composites and residual stress induced dimensional instabilities of antisymmetric composites. The effect of nanoparticle loading on the CTE of 10-ply composites with a $(0/90/0/90/0)_s$ symmetric layup will be characterized using thermomechanical analysis. It is well-known that lack of symmetry in a composite layup can lead to build up of residual stresses, which results in severe curvature or warpage of the specimen following the cure process. Hence, in this work, 2-ply samples with 0/90 antisymmetric layup were used as model systems to study the effect of nanoparticle loading on the residual stress induced warpage.

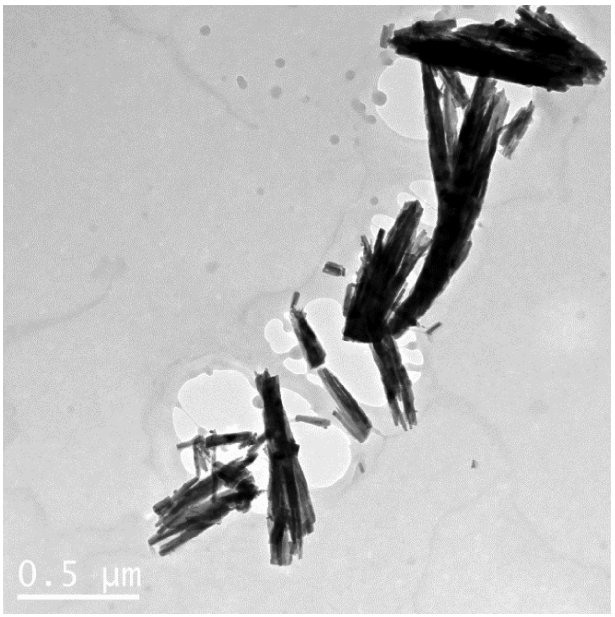

Figure 1. TEM image representing the morphology of hydrothermally synthesized ZrW_2O_8 nanoparticles.

2. EXPERIMENTAL SECTION

2.1. Materials. The BECy resin used was EX 1510 resin obtained from Tencate Technologies (Morgan Hill, CA). The catalyst (EX 1510 B) required for curing the resin was also obtained from Tencate Technologies and added at a ratio of 3 parts catalyst per hundred parts resin. The unidirectional carbon fiber mats (#2596, Intermediate Modulus (IM), 4.3 oz/sq yd, 0.006 in. thick) were obtained from FiberGlast Inc. (Brookeville, OH) and consisted of 12 K filaments per tow.

2.2. ZrW_2O_8 Nanoparticle Synthesis and Functionalization. The nanoparticles were synthesized through a hydrothermal approach,[31] which is described in detail in our recent work.[28] The ZrW_2O_8 nanoparticles were functionalized using 3-glycidyloxypropyl trimethoxysilane to improve the compatibility of the nanoparticles with the BECy polymer matrix.[32,33] The method involved replacement of the surface hydroxyl groups on the nanoparticle surface with O−Si groups using the epoxy terminated silane, and is also described in detail elsewhere.[28]

2.3. Composite Layup and Processing. In this work, 10-ply symmetric composites with a $(0/90/0/90/0)_s$ layup were prepared to characterize the effect of nanoparticle loading on the CTE measured both normal (out of plane mode) and parallel (in plane mode) to the direction of fibers. For preparing hybrid composites, a required amount of functionalized ZrW_2O_8 nanoparticles were added to the neat BECy resin and the suspension was homogenized by ultrasonic mixing using a Branson 1510 Ultrasonic Bath. For the 10-ply composites, the nanoparticle loadings were varied between 0 to 20 vol % of the resin, whereas the overall weight percent of the carbon fibers in the composite was 30 wt %. Individual plies were prepared by applying the nanocomposite suspensions with various ZrW_2O_8 loadings evenly to both sides of the carbon fiber plies. Each ply was then laid in the desired orientation on Teflon film and rolled with a lightweight plastic roller to attain complete wetting before laying the next ply. The composites were then degassed under vacuum for thirty minutes to remove air voids and bubbles. The composites were placed in a hot press and heated to 160 °C and held isothermally for a few minutes to pre cure the resin and to prevent it from flowing out of the mold under pressure. The precure time was 10 min for

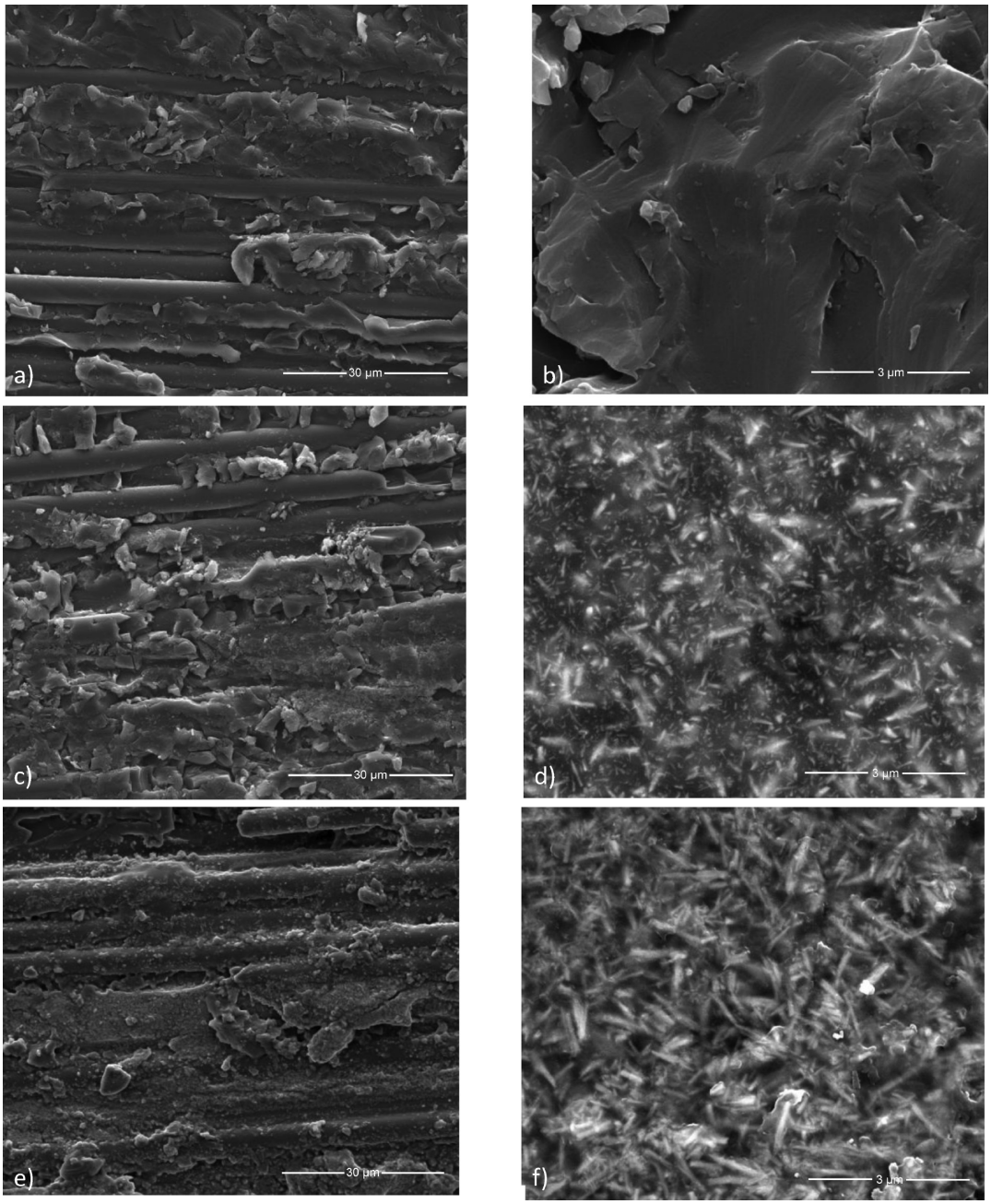

Figure 2. SEM images of symmetric 10-ply hybrid composites: (a) neat BECy/carbon fiber sample, 1500×; (b) neat BECy/carbon fiber sample, 15 000×; (c) hybrid carbon fiber composite with BECy/10 vol % ZrW_2O_8 nanocomposite matrix, 1500×; (d) hybrid carbon fiber composite with BECy/10 vol % ZrW_2O_8 nanocomposite matrix, 15 000×; (e) Hybrid carbon fiber composite with BECy/20 vol % ZrW_2O_8 nanocomposite matrix, 1500×; (f) hybrid carbon fiber composite with BECy/20 vol % ZrW_2O_8 nanocomposite matrix, 15 000×.

neat BECy resin while only 7 or 8 min of precure was required for the nanocomposite suspensions due to the catalytic effect of the ZrW_2O_8 nanoparticles. Following the short pre cure, pressure was then immediately applied and held constant at 21.75 kPa (150 psi), whereas the temperature was increased from 160 to 180 °C, where the sample was held isothermally for 2 h. The composite was then allowed to cool to room temperature still under pressure for 3 h. The pressure was completely released once the sample had attained room temperature. The composite was subsequently postcured at 250 °C for 2 h in a convection oven under a pressure plate to achieve full cure and was cooled at 1 °C/min back to room temperature, following the cure.

Thin, 2 ply composites were prepared with an antisymmetric 0/90 lay up in order to examine the effect of ZrW_2O_8 nanoparticle loading on the residual stress induced warpage. The cure schedule and processing steps were the same as those used for preparing the 10-ply composites. The nanoparticle loadings were varied between 0 and 10 vol % of the resin, whereas the overall carbon fiber content was maintained at 30 wt %, also similar to the 10-ply composites. The density of the resin, ZrW_2O_8 filler, and carbon fiber are 1.2, 5.07, and 1.75 g/cm^3, respectively.

2.4. Characterization. The morphology of the hydrothermally synthesized ZrW_2O_8 nanoparticles was characterized with a JEOL 2100 200 kV microscope. The nanoparticles were dispersed in acetone and

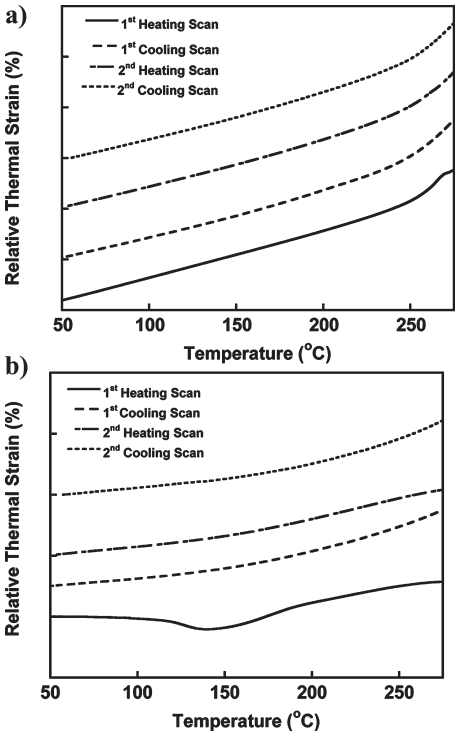

Figure 3. TMA measurements showing the effect of temperature on thermal strain profiles during sequential heating and cooling scans for (a) neat carbon fiber/BECy composite, (b) hybrid carbon fiber/BECy-20 vol % ZrW_2O_8 nanocomposite. The curves have been shifted for comparison and only relative thermal strain is shown.

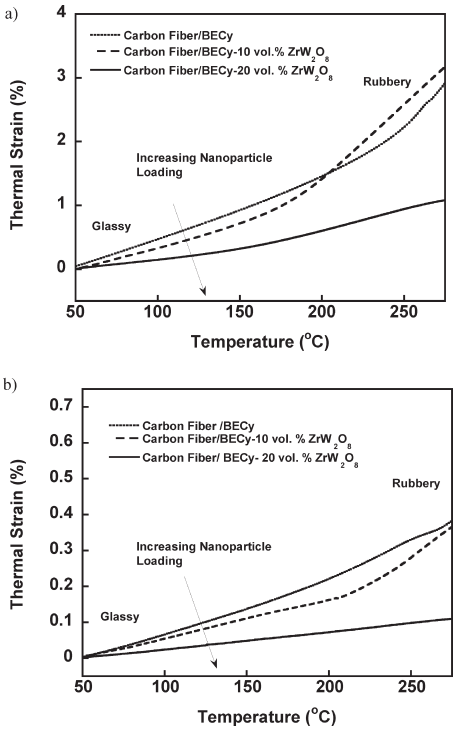

Figure 4. TMA measurements at 5 °C/min for 10-ply composites as a function of nanoparticle loading: (a) out of plane mode, (b) in plane mode.

placed in a Formvar grid for imaging. Scanning electron microscopy of the fully cured composite specimen was performed with a FEI Quanta FE SEM. Sections of the 10-ply composites were prepared for imaging using a low speed, diamond blade saw. The CTE of the 10-ply symmetric composite samples were characterized using a Q400 Thermomechanical analyzer (TMA) from TA Instruments. The thermomomechanical properties of the composites were characterized using the second heating scan of a heat/cool/heat cycle performed at 5 °C/min from 25 to 300 °C. Accurate assignment of the glass transition is easier for the second heating scan due to the absence of overshoot features near the glass transition that are present in the dimension change curves in the first heating scans. The dynamic mechanical properties of the composites were characterized using a Q800 dynamic mechanical analyzer (DMA) from TA Instruments in the three point bending mode on heating at 3 °C/min at a frequency of 1 Hz and amplitude of 5 μm.

The effect of temperature on the warpage of the 2 ply antisymmetric composites was characterized using a custom designed setup. The samples were smoothed along the edges and placed in the stage of temperature controlled oven with a clear glass window. One end of the sample was supported on the stage while the dimension change of the other end was monitored using a digital camera, which was mounted on a stand and aligned along the same level as the sample stage. The measurements were performed by heating the sample to temperatures from 50 to 300 °C at intervals of 25 °C. The sample was allowed to equilibrate at each temperature for several minutes, after which three photographs were recorded. The photographs were analyzed with image processing software to determine the variation of sample curvature with temperature. All samples were prepared with the same batch of BECy because of the tendency of BECy to crystallize during storage.

3. RESULTS

The ZrW_2O_8 nanoparticles synthesized by the hydrothermal method are characterized by whiskerlike morphology, as shown in Figure 1, with widths ranging from 50 to 200 nm and lengths of approximately 1 μm. The crystalline nanoparticles are characterized by a cubic crystal structure. More detailed discussions on the functionalization and characterization of these nanoparticles have been reported in our recent work.[28] The SEM images of the10-ply symmetric composites with various nanoparticle loadings are shown in Figure 2a—f. The images obtained at 1500× magnification (images a, c, and e) provide an overview of the macroscale carbon fibers embedded in either the neat BECy or the BECy/ZrW_2O_8 nanocomposite matrices, while the images at 15000× magnification (images b, d, and f) illustrate the distribution of the nanoparticles in the BECy matrix phase. The SEM images shown Figures 2d and 2f demonstrate that the ZrW_2O_8 nanoparticles are well-dispersed in the BECy matrix for both 10 and 20 vol % nanoparticle loadings.

The effect of temperature on the thermal strain profiles of the composites during the sequential heating and cooling measurements is shown in panels a and b in Figure 3 for the neat carbon fiber/BECy composite and the hybrid carbon fiber/BECy-20 vol % ZrW_2O_8 composite. The first heating scan for the neat composite and the hybrid composite exhibits a relaxation overshoot at the glass transition due to the thermal history experienced during the cure. For both types of composites, the slopes of the thermal strain curves vary by less than 2% during the three subsequent scans that follow the first heating scan confirming the absence of detrimental effects such as degradation during the thermal histories imposed in this work. Furthermore, in our previous work,[23] we found that the residual stresses developed during the cure of BECy resin reinforced with bulk ZrW_2O_8 were

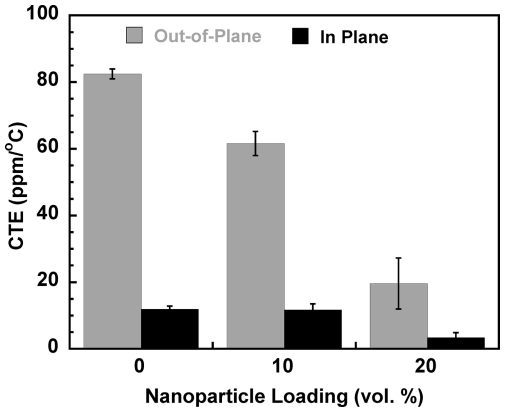

Figure 5. Effect of nanoparticle loading on the CTE of 10-ply hybrid composites in the out of plane and in plane modes of measurement. Error bars are standard deviations based on three or four measurements for each sample.

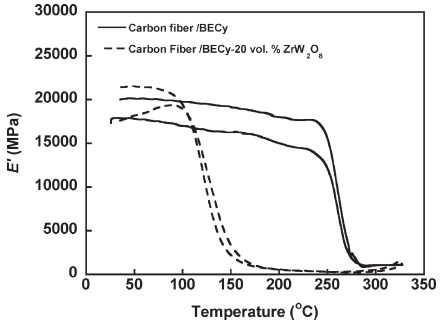

Figure 6. Effect of nanoparticle loading on the dynamic mechanical properties of carbon fiber/BECy composites.

sufficient to induce formation of the gamma phase, which has a lower magnitude of negative CTE when compared to the cubic α phase. This was confirmed by the fact that the samples with high loadings of bulk ZrW_2O_8 (65 vol %) exhibited an irreversible gamma−alpha transition at 120 °C during the first heating scan, which was accompanied by a large increase in thermal strain. However, the first heating scan for the hybrid composites prepared in this work do not exhibit any large increase in thermal strain, suggesting that ZrW_2O_8 nanoparticles were not transformed to gamma phase during the cure.

The thermal expansion behavior of the 10-ply symmetric composites was characterized in two measurement modes. In the out of plane mode, the samples were placed on the TMA sample stage such that all the plies were aligned normal to the TMA probe, whereas for the in-plane mode, the sample was placed on the sample stage some of the plies were aligned parallel to the probe direction. The measurements could be performed with either 4 or 6 plies parallel to probe direction; however, no significant or systematic differences were observed based on whether 4 or 6 plies were aligned parallel to the probe. The thermal strain curves obtained on heating 5 °C/min are compared as a function of nanoparticle loading for the out of plane and in plane measurement modes in panels a and b in Figure 4, respectively. In general, the thermal strain curves exhibit a change in slope with increasing temperature because of the onset of the glass transition, which signals a transformation of the material

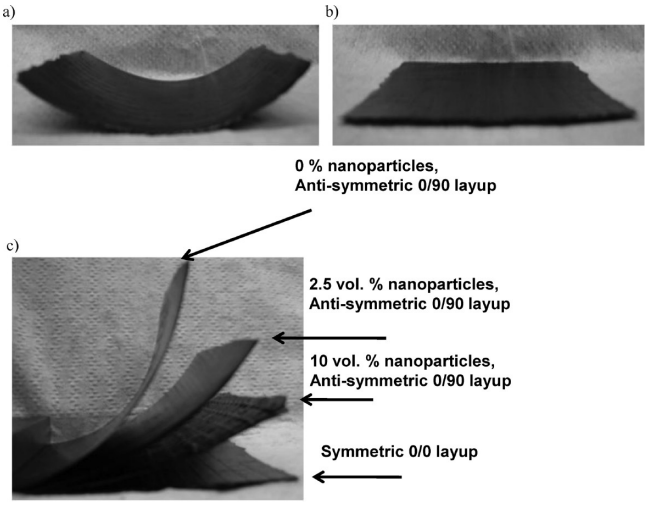

Figure 7. (a) 2-Ply composite with antisymmetric 0/90 layup, (b) 2-ply composite with symmetric 0/0 layup, (c) Effect of ZrW_2O_8 nanoparticle loading on the curvature or warpage of 2-ply antisymmetric composites. The composites were supported along one edge for comparison. A flat 2-ply symmetric composite (0/0 layup) is included in the comparison as a reference.

from a rigid glassy state to a rubbery state. Furthermore, for both out of plane and in plane measurements, the magnitude and the slope of the thermal strain curves decreases dramatically with ZrW_2O_8 nanoparticle loading, as shown in panels a and b in Figure 4.

The values of CTE (α) can be determined from the slope of the thermal strain curves, as shown in eq 1 below

$$\alpha = \frac{1}{L_0}\frac{dL}{dT} \quad (1)$$

Where L_o is the original sample length and dL/dT is the change in sample length with change in temperature. The values of α calculated in the glassy region (from 50 to 100 °C) based on a linear regression of the data are plotted as a function of nanoparticle loading in Figure 5 for both modes. In the out of plane mode, CTE decreases significantly with increasing ZrW_2O_8 nanoparticle loading. The CTE of the carbon fiber/BECy-20 vol % ZrW_2O_8 hybrid composite is 76% lower than the CTE of carbon fiber/neat BECy composite. For any level of nanoparticle loading, the absolute values of CTE are lower for measurements from the in plane mode when compared to the measurements in the out of plane mode. This is not unexpected since the CTE of carbon fiber is usually between 7×10^{-6} and 10×10^{-6} K^{-1} in the normal direction and between -0.5×10^{-6} and -1.4×10^{-6} K^{-1} in the parallel or in-plane direction.[34] In the in-plane mode, the maximum decrease in CTE is found to be 72% for the carbon fiber/BECy-20 vol % ZrW_2O_8 hybrid composite in comparison to the carbon fiber/neat BECy composite. Furthermore, the dramatic CTE reduction as a consequence of nanoparticle loading results in a very low or near zero thermal expansion (3.4 ppm/°C) for the composites in the in-plane mode. These significant CTE reductions demonstrate the potential for development of composites with tailored CTE values through incorporation of ZrW_2O_8 nanoparticles.

Apart from a reduction in CTE, the thermal strain curves shown in Figure 4 also suggest a systematic decrease in the onset of the glass transition temperature of the composites with increasing nanoparticle loading. For, example, the average value

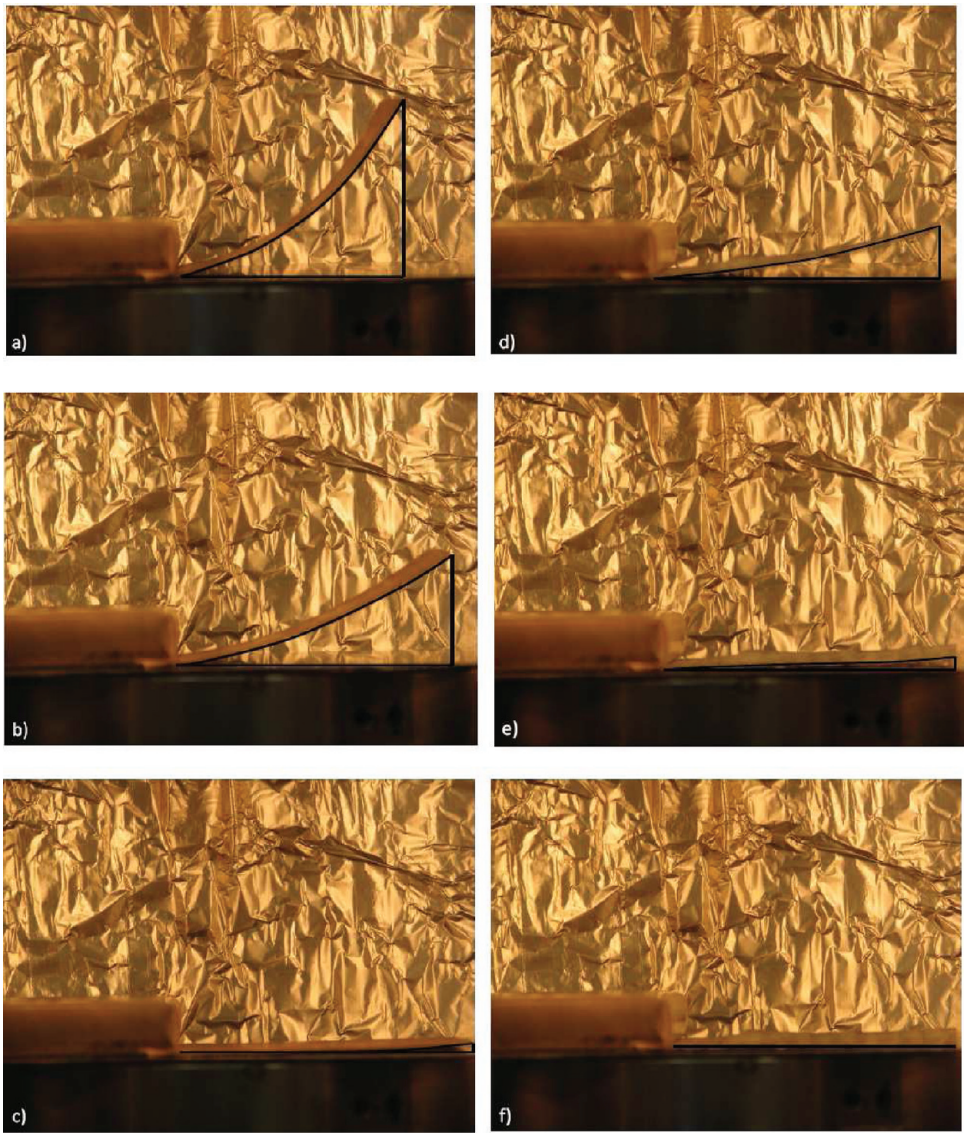

Figure 8. Effect of temperature on curvature of 2-ply antisymmetric composites a) T = 50 °C, carbon fiber/neat BECy composite; (b) T = 150 °C, carbon fiber/neat BECy; (c) T = 300 °C, carbon fiber/neat BECy; (d) T = 50 °C, carbon fiber/BECy −10 vol.% ZrW_2O_8 e) T = 150 °C, carbon fiber/BECy −10 vol % ZrW_2O_8; (f) T = 300 °C, carbon fiber/BECy −10 vol % ZrW_2O_8. The edges and change in vertical and horizontal displacements are illustrated in all images using black lines as a guide to clearly illustrate the change in curvature with temperature.

of T_g, measured as point of intersection of glassy and liquid lines in Figure 4a, is found to decrease from 249.3 ± 2.5 °C for the carbon fiber/neat BECy composite to 151.1 ± 1.9 °C for the carbon fiber/BECy-20 vol % ZrW_2O_8 hybrid composite. In our previous work,[28] DSC measurements revealed that the cure of BECy/ZrW_2O_8 nanocomposites was characterized by the presence of an additional low temperature exotherm, indicative of side reactions as a consequence of the surface hydroxyl groups present in the ZrW_2O_8 nanocomposites. Silane functionalization mitigated the extent of the side reactions, as evident from a reduction in the magnitude of the low-temperature exotherm; however, they are not completely eliminated as not every hydroxyl group on the nanoparticle surface can be functionalized. These side reactions may lead to chemical and physical changes in the cross-linked structure of BECy, which manifests in the form a reduced T_g value. The decrease in T_g observed in TMA measured is also confirmed through DMA measurements, which reveal a shift in the onset temperatures to lower values upon incorporation of ZrW_2O_8 nanoparticles, as shown in Figure 6. However, no significant detrimental effect is observed on the dynamic storage modulus (E') of the composites, as a consequence of nanoparticle loading.

In spite of the T_g reductions following incorporation of ZrW_2O_8 nanoparticles, the hybrid composites developed in this work are good candidates for high-performance applications because they are characterized by T_g values higher than 150 °C, high stiffness, and low values of CTE.

The use of BECy/ZrW_2O_8 nanocomposites to reduce the mismatch in CTE between the polymer matrix and the low CTE carbon fibers in the hybrid composite systems can provide direct benefits in terms of a reduction in the magnitude of thermally induced stress both upon cooling the material following the cure and during subsequent thermal cycling. The effect of layup symmetry on the shape of the composite following the cure is

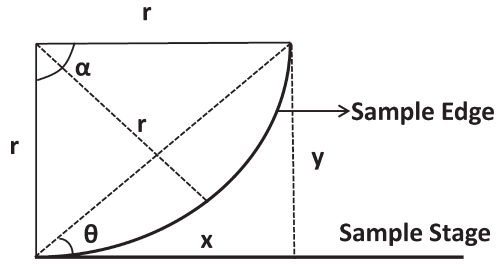

Figure 9. Schematic representation of curvature measurement for 2-ply antisymmetric composites.

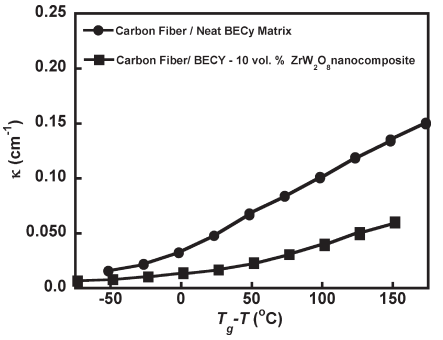

Figure 10. Relationship between curvature, nanoparticle loading, and temperature for 2-ply antisymmetric composites. On the basis of TMA measurements, the T_g for the 2-ply composites with neat BECy matrix and BECy/10 vol % ZrW_2O_8 nanocomposite matrix was 248.3 and 176.5 °C, respectively.

demonstrated in images a and b in Figure 7, which shows that an initially flat neat BECy/carbon fiber composite sample with antisymmetric (0/90) layup is curved or warped upon cooling down following the cure, as shown in Figure 7a; however, a neat BECy/carbon fiber composite sample with a symmetric (0/0) layup remains flat after the same cure schedule, as shown in Figure 7b. In the case of the antisymmetric sample, the buildup of residual stresses arising from the lack of symmetry leads to a completely warped specimen upon cooling the sample following the cure process. Interestingly, incorporation of ZrW_2O_8 nanoparticles results in a significant reduction in curvature or warpage of the 2-ply antisymmetric composite specimen following the cure, as shown in Figure 7c.

The residual stresses (σ_r) generated in a constrained polymer composite at a given temperature can be expressed as shown in eq 2 below

$$\sigma_r \propto (T_g - T)\alpha_c \tag{2}$$

where, T is temperature of interest and α_c is the CTE of the composite. Upon incorporation of 10 vol % nanoparticles in the BECy matrix, the CTE of a 2-ply symmetric composite is reduced by 28% in comparison to the carbon fiber/neat BECy composite. However, the T_g of the 2-ply composite is also reduced significantly from 248.3 °C for the carbon fiber/neat BECy composite to 176.5 °C for the carbon fiber/BECy-10 vol % ZrW_2O_8 hybrid composite, similar to the results shown in Figure 4 for the 10-ply composites. In general, a composite material does not experience significant residual stress at temperatures above the T_g of the polymer matrix where stresses can relax with time, but the stresses start developing as the materials cools down to temperatures below the T_g. Consequently, apart from a reduction in CTE, a reduction in T_g could also mitigate the extent of warpage developed in the composite through a reduction in the temperature window available for development of residual thermal stresses. Hence, the effects of CTE reduction and T_g reduction need to be delineated in order to better understand the decrease in warpage exhibited by the antisymmetric hybrid composites in Figure 7b.

The effect of temperature on the curvature of antisymmetric BECy/carbon fiber composite is illustrated through the images in Figure 8a−c. As the temperature is increased, the curvature of the composite decreases and the sample becomes flatter once the residual stresses are relieved above the glass transition, as illustrated in Figure 8c. Upon cooling the sample from 300 °C, the residual stresses develop once again, leading to a warped sample at room temperature. At any temperature, the hybrid composite with the BECy/10 vol % ZrW_2O_8 nanocomposite matrix exhibits lower curvature in comparison to the composite with the neat BECy matrix, as shown in Figure 8d−f.

The photographs obtained at various temperatures for the neat composite and the hybrid composite were analyzed to determine the curvature of the composite specimen, as shown in Figure 9. The composite panel when clamped along one edge on a stage could be considered as an arc of length L in a segment of radius r. The angle of curvature (θ) can be measured from the ratio of vertical distance (y) and horizontal distance (x), which was determined from image processing software. The angle of the composite segment (α) can be determined by solving for eq 3 shown below

$$\frac{1 - \cos\alpha}{\sin\alpha} = \tan\theta \tag{3}$$

The radius of the segment is determined as $r = L/\alpha$, where L is the length of the sample (7.9 cm). The curvature (κ) of the sample can be obtained as $\kappa = 1/r$. It is acknowledged that the method used in this work only facilitates estimation of the overall curvature of the composite specimen and does not account for local changes or variations in curvature across the ply. Such changes may be captured using more advanced techniques such as laser profilemetry or motion capture techniques.[35] However, since the goal of this study was only to separate the effect of CTE reduction from T_g reduction, as discussed earlier, the measurement of an overall change in κ can be considered adequate.

The relationships between κ and the temperature window below T_g (defined as $T_g - T$) is compared for the antisymmetric composites with and without nanoparticles in Figure 10. At temperatures higher than T_g, ($T_g - T$) is negative and the curvature values approach zero because of the presence of minimal or no residual stress. On the other hand, at temperatures lower than T_g, the curvature increases systematically with decreasing temperature, as expected. Figure 10 demonstrates that replacement of the neat BECy matrix with the BECy/10 vol % ZrW_2O_8 nanocomposite results in lower curvature at any value of ($T_g - T$). In other words, for the same distance from the glass transition, the hybrid composite is characterized by lower magnitude of curvature. Hence, the reduction in the CTE mismatch between the carbon fibers and the polymer matrix achieved through incorporation of nanoparticles plays a significant role in reducing the curvature for the hybrid composites.

The results from this work show that the CTE of traditional carbon fiber reinforced composite systems can be successfully tailored through incorporation of negative CTE ZrW_2O_8 nanoparticles. The ability to tailor the CTE of composite systems to

match the CTE of surfaces and substrates that they may operate in contact with could potentially minimize manifestations of residual stress induced issues such as matrix microcracking or delamination. A reduction in the mismatch of CTE between the polymer matrix and the fiber reinforcements can also facilitate fabrication of components with better dimensional stability and improved service lifetimes.

4. CONCLUSIONS

In this work, novel carbon fiber reinforced BECy/nano-ZrW_2O_8 composite laminates were fabricated. TMA measurements of 10-ply composite specimen with symmetric layup indicated that a CTE reduction of up to 76% could be attained with 20 vol % ZrW_2O_8 nanoparticle loading in the out of plane mode along with a 72% reduction in the out of plane mode. For a nanoparticle loading of 20 vol %, the composites exhibited very low or near zero thermal expansion in the in plane mode. However, for both in-plane and out-of-plane modes, the reduction in CTE was accompanied by a reduction in the glass transition, which was not overcome even after silane surface functionalization of the particles. The residual stress-induced warpage of 2-ply antisymmetric composites was systematically reduced upon incorporation of ZrW_2O_8 nanoparticles. Because either a reduction in CTE or a reduction in the onset of the glass transition could reduce warpage following thermoset cure, the relationship between nanoparticle loading and curvature was examined at various temperatures. The study revealed that the CTE reduction plays a significant role in the reduction of curvature for the hybrid composites since at any given distance from the glass transition, the hybrid composite specimen exhibited lower curvature than a composite specimen that did not contain any nanoparticles. The ability to tailor the CTE of fiber reinforced composite systems and to reduce the CTE mismatch between the fiber reinforcements and the matrix could minimize residual stresses during thermal cycling, facilitate manufacturing of composite components with precise dimensions, and improve the service lifetimes of advanced composite systems.

AUTHOR INFORMATION

Corresponding Author

*E-mail: mkessler@iastate.edu.

ACKNOWLEDGMENT

This work was funded by the Air Force Office of Scientific Research under award no. FA 9550-08-1-0033. This work was also supported in part by National Science Foundation Research Experience for Undergraduates (NSF DMR REU Site 0755231). Support for MKR from the Department of Energy's, Science Undergraduate Laboratory Internship program is also acknowledged. The author's acknowledge Hongchao Wu (Materials Science and Engineering, Iowa State University) for his assistance with SEM measurements.

REFERENCES

(1) Lange, J.; Toll, S.; Manson, J. E.; Hult, A. *Polymer* **1995**, *36*, 3131.
(2) Cowley, K. D.; Beaumont, P. W. R. *Compos. Sci. Technol.* **1997**, *57*, 1445.
(3) Thostenson, E. T.; Li, W. Z.; Wang, D. Z.; Ren, Z. F.; Chou, T. W. *J. Appl. Phys.* **2002**, *91*, 6034.
(4) Veedu, V. P.; Cao, A.; Li, X.; Ma, K.; Soldano, C.; Kar, S.; Ajayan, P. M.; Mehrdad Nejhad, M. N. *Nat. Mater.* **2006**, *5*, 457.
(5) Lin, Y.; Ehlert, G.; Sodano, H. A. *Adv. Func. Mater.* **2009**, *19*, 2654.
(6) Kim, M.; Park, Y. B.; Okoli, O. L.; Zhang, C. *Compos. Sci. Technol.* **2009**, *69*, 35.
(7) Gojny, F. H.; Wichmann, M. H. H.; Fiedler, B.; Bauhofer, W.; Schulte, K. *Compos. Part A. Appl. S.* **2005**, *36*, 1525.
(8) Qiu, J.; Zhang, B.; Wang, B.; Liang, R. *Nanotechnology* **2007**, *18*, 275708.
(9) Kim, M. T.; Rhee, K. Y.; Lee, J. H.; Hui, D.; Lau, A. K. T. *Compos. Part B. Eng.* **2011**, *42*, 1257.
(10) Inam, F.; Wong, D. W. Y.; Kuwata, M.; Peijs, T. *J. Nanomater.* **2010**, *453420*, DOI: 10.1155/2010/453420.
(11) Zhang, G.; Karger-Kocsis, J.; Zou, J. *Carbon* **2010**, *48*, 4829.
(12) Green, K. J.; Dean, D. R.; Vaidya, U. K.; Nyairo, E. *Composites, Part A* **2009**, *40*, 1470.
(13) Tzantzalis, S.; Karapappas, P.; Vavouliotis, A.; Tsotra, P.; Paipetis, A.; Kostopoulos, V.; Friedrich, K. *Composites, Part A* **2007**, *7*, 1076.
(14) Dean, D.; Obore, A. M.; Richmond, S.; Nyairo, E. *Compos. Sci. Technol.* **2006**, *66*, 2135.
(15) Wichmann, M. H. G.; Sumfleth, J.; Gojny, F. H.; Quaresimin, M.; Fiedler, B.; Schulte, K. *Eng. Fract. Mech.* **2006**, *73*, 2346.
(16) Chowdhury, F. H.; Hosur, m.v.; Jeelani, S. *Mater. Sci. Eng. Struct.* **2006**, *421*, 298.
(17) Mary, T. A.; Evans, J. S. O.; Vogt, T.; Sleight, A. W. *Science* **1996**, *61*, 275.
(18) Sleight, A. W. *Annu. Rev. Mater. Sci.* **1998**, *28*, 29.
(19) Evans, J. S. O.; Jorgensen, J. D.; Short, S.; David, W. I.; Ibberson, R. M.; Sleight, A. W. *Phys. Rev. B.* **1999**, *60*, 14643.
(20) Miller, W.; Smith, C. W.; Dooling, P.; Burgess, A. N.; Evans, K. E. *Phys. Stat. Sol. B.* **2008**, *245*, 552.
(21) Shi, J. D.; Pu, Z. J.; Wu, K. H.; Larkins, G. *Proc. Mat. Res. Soc. Symp.* **1997**, 229.
(22) Tani, J. I.; Kimura, H.; Hirota, K.; Kido, H. *J. Appl. Polym. Sci.* **2007**, *106*, 3343.
(23) Badrinarayanan, P.; Macmurray, B.; Kessler, M. R. *J. Mater. Res.* **2009**, *24*, 2235.
(24) Goertzen, W. K.; Kessler, M. R. *J. Therm. Anal. Calorim.* **2008**, *93*, 87.
(25) Weyer, W. C.; Cross, W. M.; Henderson, B.; Kellar, J. J.; Kjerengtroen, L.; Welsh, J.; Starkovich, J. In *Proceedings of the 46th AIAA/ASME/ASCE/AHS/ASC Structures, Structural Dynamics & Materials Conference*; Austin, TX, Apr 18−21, 2005; AIAA: Reston, VA, 2005; p 3577.
(26) Sullivan, L. M.; Lukehart, C. M. *Chem. Mater.* **2005**, *17*, 2136.
(27) Lind, C.; Coleman, M. R.; Kozy, L. C.; Sharma, G. R. *Phys. Status Solidi B* **2011**, *248*, 123.
(28) Badrinarayanan, P.; Kessler, M. R. *Compos. Sci. Technol.* **2011**, *71*, 1385.
(29) Goertzen, W. K.; Kessler, M. R. *Composites, Part A* **2007**, *38*, 779.
(30) Sheng, X.; Akinc, M.; Kessler, M. R. *J. Therm. Anal. Calorim.* **2008**, *92*, 77.
(31) Kozy, L. C.; Tahir, M. N.; Lind, C.; Tremel, W. *J. Mater. Chem.* **2009**, *19*, 2760.
(32) Sheng, X.; Akinc, M.; Kessler, M. R. *Polym. Eng. Sci.* **2010**, *50*, 302.
(33) Haman, K. J.; Badrinarayanan, P.; Kessler, M. R. *ACS App. Mat. Int.* **2009**, *1*, 1190.
(34) Karadeniz, Z. H.; Kumlutas, D. *Compos. Struct.* **2007**, *781*, 1.
(35) Giddings, P. F.; Bowen, C. R.; Salo, A. I. T.; Kim, H. A.; Ive, A. *Compos. Struct.* **2010**, *92*, 2220.